ACS Macro Letters

Letter

Cite This: ACS Macro Lett. 2019, 8, 540−545

pubs.acs.org/macroletters

Synthesis and High Alkaline Chemical Stability of Polyionic Liquids with Methylpyrrolidinium, Methylpiperidinium, Methylazepanium, Methylazocanium, and Methylazonanium Cations

Rui Sun and Yossef A. Elabd*

Department of Chemical Engineering, Texas A&M University, College Station, Texas 77843, United States

Supporting Information

ABSTRACT: Herein, we present the synthesis of five styrene-based poly(ionic liquids) (PILs) containing (covalently linked) saturated *N*-heterocyclic cations with various ring sizes (i.e., methylpyrrolidinium, methylpiperidinium, methylazepanium, methylazocanium, and methylazonanium). High alkaline chemical stability was confirmed by ^{1}H NMR spectroscopy after 4 weeks in 40 mol equiv of KOH (1.0 M KOH in D_2O) at 80 °C for PILs with 5-, 6-, 7-, and 8-membered ring cations; a requirement for polymer electrolyte separators in long-lasting alkaline fuel cells. Additionally, ion conductivity of PILs increased by 4 orders of magnitude with increasing water content, where a master percolation power law curve was observed, that is, similar conductivity versus water volume fraction for all PILs, regardless of cation size.

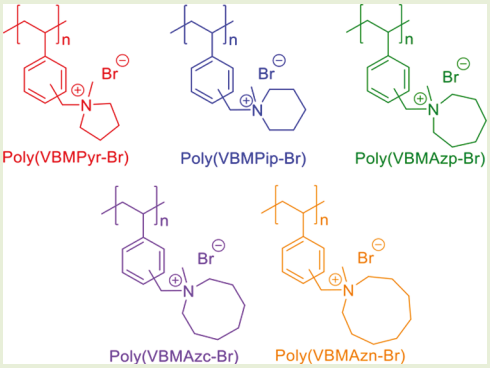

Alkaline fuel cells (AFCs) utilizing solid-state anion exchange membranes (AEMs) as electrolyte separators have recently attracted significant interest for several reasons: (1) the potential to achieve high fuel cell power densities at a lower cost compared to proton exchange membrane fuel cells (PEMFCs) with the use of non-noble metal catalysts (e.g., nickel, silver, etc.) and (2) the potential to improve fuel cell lifetimes compared to liquid electrolytes by preventing caustic electrolyte leakage and potassium carbonate/bicarbonate precipitation.[1,2] To achieve high power density and long-term durability, a desirable AEM candidate requires high alkaline chemical stability (due to the high nucleophilicity and basicity of the hydroxide ions as charge carriers), as well as sufficient ion transport. Various AEMs have been developed and investigated as solid-state electrolytes in AFCs.[3−13] However, to date, there is no commercially available solid-state AEM that exhibits excellent alkaline chemical stability, which is required for long-lasting AFC performance. Therefore, synthesis and exploration of new chemistries is of significant importance to improve the chemical stability of AEMs and subsequently promote the commercialization of AFCs.

Several studies have investigated the degradation of AEM chemistries, suggesting that both the polymer backbone (e.g., poly(phenylene oxide),[14] polysulfone,[15] etc.) and the covalently attached cation group (e.g., acyclic quaternary ammonium (QA),[16] imidazolium,[17,18] etc.) have a profound impact on the alkaline chemical stability.[19−22] For example, Mohanty et al.[19] compared various polymer backbones with tetramethylammonium (TMA) cations and found that aromatic polymers without aryl ether bonds possessed the highest chemical stability. Meek et al.[22] also reported higher chemical stability of styrene-based backbone compared to acrylate-based backbones. Regarding the cation groups, QA cations have been extensively investigated and shown to degrade via Hoffman elimination (E_2), nucleophilic substitution (S_N2), and ylide formation, under highly basic conditions.[3,13,23] Ye et al.[17] reported the enhanced chemical stability of poly(ionic liquids) (PILs) containing unsaturated imidazolium cations compared to benchmark TMA cations, attributed to the presence of the π-conjugated structure and the steric hindrance offered by the five-membered heterocyclic ring. However, multiple studies have shown that the degradation of imidazolium will still be triggered by the high nucleophilicity and basicity of OH^- ions under vigorous conditions and will undergo a ring opening degradation mechanism.[17,21,22]

Recent studies have shown higher alkaline chemical stability for polymers bearing a saturated *N*-heterocyclic cation (i.e., pyrrolidinium) versus acyclic QA cations and unsaturated imidazolium cations, partially attributed to the nonpolarizable pyrrolidinium ring.[5,9,21,22] Additionally, several studies on small molecules have reported increasing stability with increasing saturated *N*-heterocyclic cation size.[24−26] However, to date, studies on saturated *N*-heterocyclic cations have almost exclusively explored smaller ring sizes (pyrrolidinium,[5,9] piperidinium[7,11,12]).

In this study, we report the synthesis of styrene-based PILs with various covalently attached cations (i.e., methylpyrrolidinium, methylpiperidinium, methylazepanium, methylazoca-

Received: January 15, 2019
Accepted: April 25, 2019

DOI: 10.1021/acsmacrolett.9b00039
ACS Macro Lett. 2019, 8, 540−545

Scheme 1. Synthesis of PILs with Various Saturated *N*-Heterocyclic Cation Ring Sizes

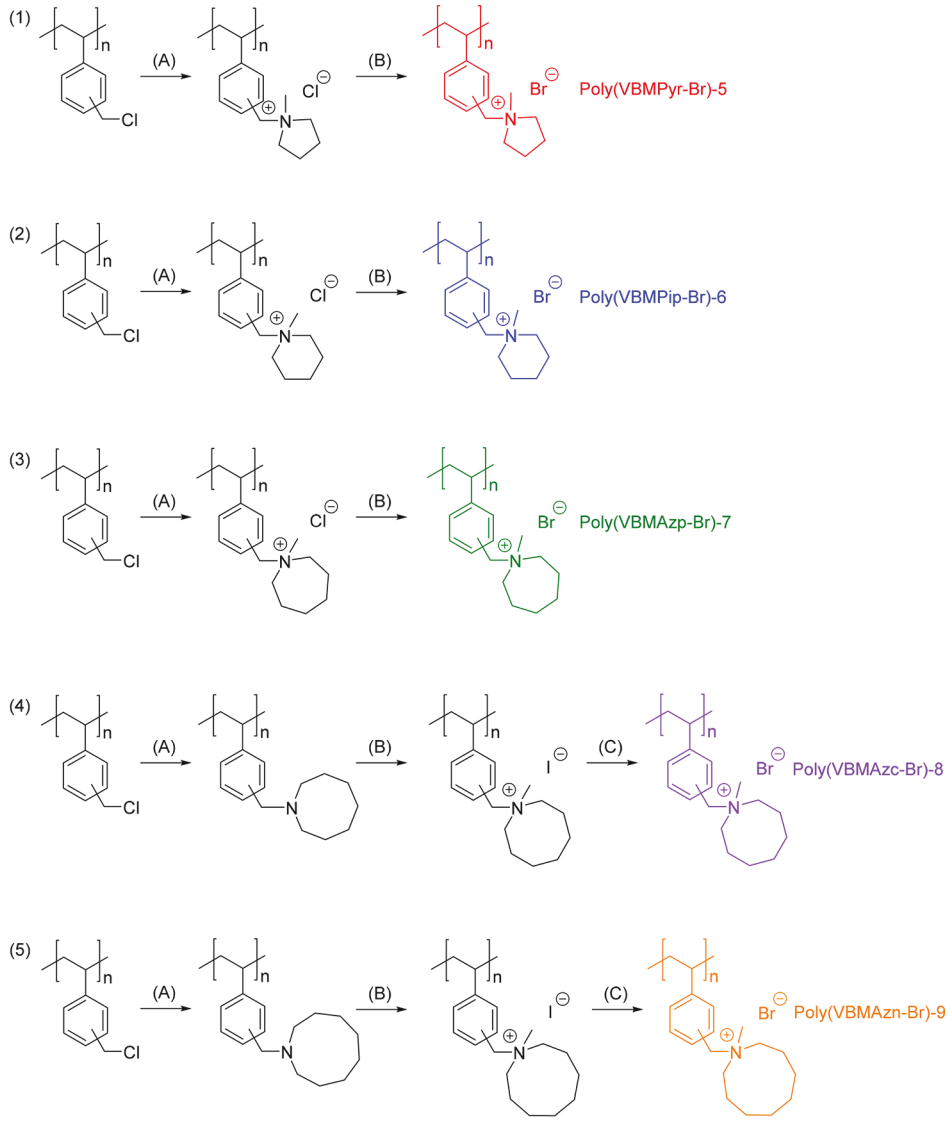

(1A) methylpyrrolidine, DMF, 65 °C, 96h; (1B) LiBr, acetone, room temperature; (2A) methylpiperidine, DMF, 80 °C, 48h; (2B) LiBr, acetone, room temperature; (3A) methylazepane, DMF, 80 °C, 48h; (3B) LiBr, acetone, room temperature; (4A) azocane, DMF, 80 °C, 48h; (4B) iodomethane, methanol, room temperature; (4C) LiBr, acetone, room temperature; (5A) azonane, DMF, 80 °C, 48h; (5B) iodomethane, methanol, room temperature; (5C) LiBr, acetone, room temperature

nium, and methylazonanium). Alkaline chemical stability, ion conductivity, and water uptake of these PILs were measured by proton nuclear magnetic resonance (^{1}H NMR) spectroscopy, electrochemical impedance spectroscopy (EIS), and dynamic vapor sorption (DVS), respectively.

Styrene-based PILs with various covalently attached saturated *N*-heterocyclic cations (methylpyrrolidinium, methylpiperidinium, methylazepanium, methylazocanium, and methylazonanium) were synthesized as novel building blocks for anion exchange membranes (Scheme 1). To covalently attach the cations onto the polymer backbone, functionalization of a nonionic polymer precursor, poly(vinylbenzyl chloride) (PVBC), was employed by two different synthesis pathways. For polymers with 5-, 6-, and 7-membered ring cations (poly(VBMPyr-Br)-5, poly(VBMPip-Br)-6, and poly(VBMAzp-Br)-7, respectively), the cationic groups (methylpyrrolidinium, methylpiperidinium, methylazepanium) were directly introduced onto the polymer backbones using methyl-substituted tertiary cyclic amines (*N*-methylpyrrolidine, *N*-methylpiperidine, and *N*-methylazepane, respectively), similar to a procedure described in previous work.[27] For polymers with 8- and 9-membered ring cations (poly(VBMAzc-Br)-8 and poly(VBMAzn-Br)-9), the cation groups (methylazocanium, methylazonanium) were introduced onto the polymer backbone using two steps. Cyclic secondary amines (azocane and azonane) were first employed to displace the chloride atom from the polymer backbone followed by a quaternization reaction with iodomethane to form the 8- and 9-membered ring cation PILs. Solid-state anion exchange metatheses with lithium bromide were then employed to achieve PILs with bromide counter anion. The chemical structure and purity of the PILs were evaluated by ^{1}H NMR spectroscopy (Figure 1) and elemental analysis (EA). The ^{1}H NMR spectra indicated the presence of methylene and methyl groups of the cations

DOI: 10.1021/acsmacrolett.9b00039
ACS Macro Lett. 2019, 8, 540−545

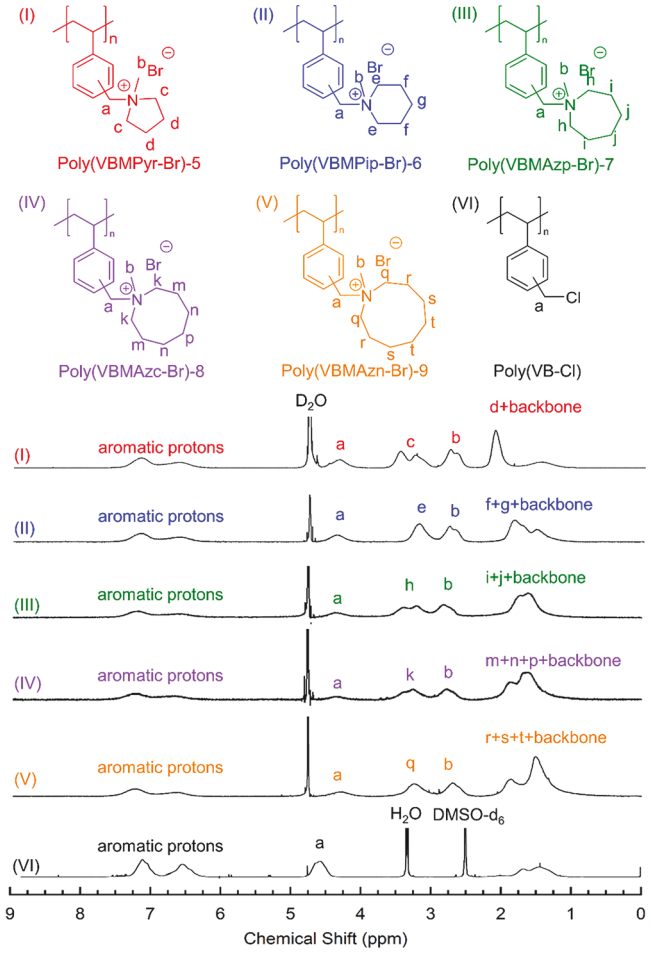

Figure 1. ^{1}H NMR spectra of PILs: (I) poly(VBMPyr-Br)-5, (II) poly(VBMPip-Br)-6, (III) poly(VBMAzp-Br)-7, (IV) poly(VBMAzc-Br)-8, (V) poly(VBMAzn-Br)-9, and (VI) poly(VB-Cl).

(covalently attached to nitrogen atom) at chemical shift positions of 2.4−3.7 ppm in all PILs, confirming the success of the functionalization reactions. The degree of functionalization was calculated by the integration ratio of CH_2 and CH_3 protons of the cations (2.4−3.7 ppm) to the aromatic protons (6.1−7.7 ppm), where all PILs were confirmed to be fully functionalized. Furthermore, the efficacy of the anion exchange metathesis was confirmed by EA (Supporting Information, S1.2−S1.6), where the compositions of the anion exchanged PILs closely match the theoretical compositions, and the chloride/iodide residues were negligibly small, indicating that the anion exchange metatheses were successful and highly efficient. Thermal properties of the PILs are shown in the Supporting Information (Figure S1), where no glass transition temperature was measurable in all PILs in the bromide form, and similar degradation temperatures (between 220−250 °C) were observed for the PILs. A more detailed synthesis procedure and experimental methods are described in the Supporting Information.

The effect of alkaline media on chemical stability was investigated by exposing the bromide-conducting PILs to high pH (40 mol equiv (1.0 M) of KOH/D_2O) at 80 °C for 4 weeks, followed by reexamining the chemical structure via ^{1}H NMR. The bromide-conducting PILs were considered to be fully hydroxide-exchanged during the alkaline chemical stability evaluation due to the excess of hydroxide anions (40 mol equiv) and therefore were not pre-exchanged to the hydroxide form. Note that a small portion of the PILs precipitated as white solid immediately after the addition of KOH/D_2O due to the partial solubility of the polymers in highly concentrated basic solution. Figure 2 shows the ^{1}H NMR spectra of each PIL after a 4-week exposure to 40 mol equiv of KOH/D_2O at 80 °C. Outstanding alkaline chemical stability was observed for PILs with 5-, 6-, and 7-membered ring cations (poly(VBMPyr-Br)-5, poly(VBMPip-Br)-6, poly(VBMAzp-Br)-7, respectively), where no evidence of cation degradation was observed in the spectra. The relative integration ratio of the cation peaks to the aromatic proton peak remained constant. There is no indication of nucleophilic substitution (S_N2) at the benzyl position of these PILs, which has been observed for the benchmark trimethylammonium (TMA) cation with the same styrene-based backbone, possibly due to the nonpolarizable nature of saturated heterocyclic ring structure, which offers higher alkaline chemical stability than TMA cations.[22] For the PIL with an 8-membered ring cation, poly(VBMAzc-Br)-8, the integration of the methylazocanium cation peak compared to the aromatic protons reduced by 2.2%, indicating a small measurable degradation of the cation. For the PIL with a 9-membered ring cation, poly(VBMAzn-Br)-9, new peaks were observed at 2.77 and 3.19 ppm and a reduction in the integration of the methylazonanium cation peak compared to the aromatic protons was also noticed. The degree of degradation of the cation was calculated to be a 22.2% decrease of the relative integration of the covalently attached methylazonanium cation to the aromatic protons. As a result, the chemical stability of the cations follows the following order: MPyr = MPip = MAzp > MAzc > MAzn. More concentrated alkaline media (80 equiv (2.0 M) and 200 equiv (5.0 M) of KOH/D_2O) were also explored in the hope to induce degradation in all PILs and explore their subsequent degradation mechanisms. However, 2.0 M experiments were similar to 1.0 M experiments, whereas complete precipitation of the PILs was observed for the 5.0 M experiments due to the solubility limit of the PILs (i.e., no peaks were observed in the NMR spectra). The white precipitate was analyzed by ^{1}H NMR spectroscopy, no change in the spectra was observed, and the white precipitate was readily redissolved back into water (Supporting Information, Figure S2). The high alkaline chemical stability can be attributed to multiple reasons, including the higher basicity of cyclic cations compared to tetramethylammonium and the geometric constraint of the cyclic structures that disfavors ring-opening elimination and ring-opening substitution.[28,29] The lower stability of the larger cations may be attributed to the higher ring strain (6-membered ring has the lowest ring strain among the cations involved in this study), which may lower the transition state energy of the degradation via elimination and subsitituion.[29,30]

In addition to the high alkaline chemical stability, the ion conductivity and water uptake of the AEM can have a significant impact on the AFC performance. In this study, the conductivity of the PILs were measured in bromide anion form; measurements in hydroxide anion form can be problematic due to the carbonation of hydroxide anions under noninert atmospheres. Figure 3a and 3b show the bromide ion conductivity and water uptake, respectively, of PILs with various cations as a function of temperature at a constant relative humidity (RH) of 90% RH. The conductivity (Figure 3a) increases with increasing temperature (30 to 80 °C) at 90% RH and follows an Arrhenius behavior with

DOI: 10.1021/acsmacrolett.9b00039
ACS Macro Lett. 2019, 8, 540−545

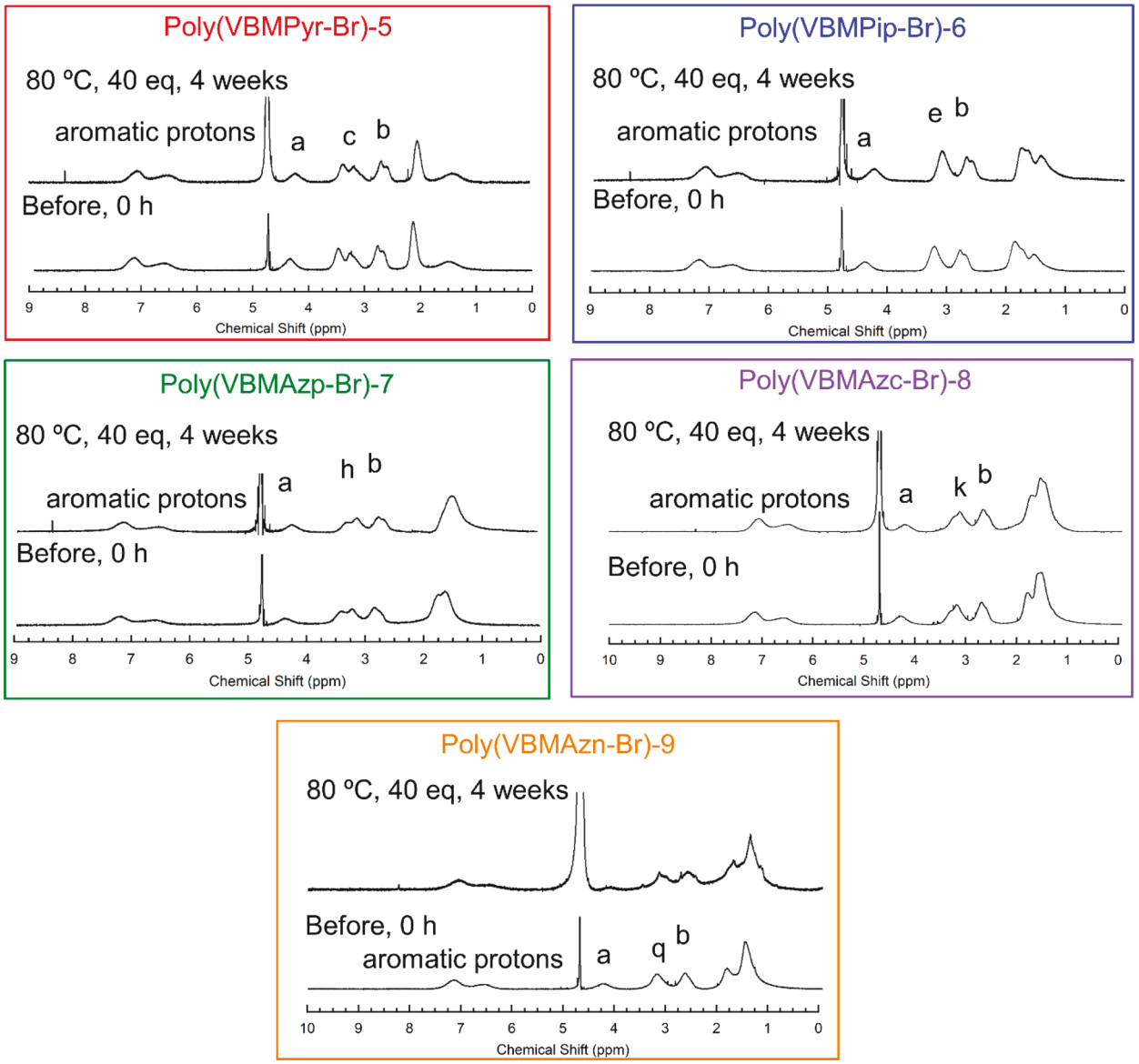

Figure 2. ^{1}H NMR spectra for PILs exposed to 40 mol equiv (1.0 M) of KOH/D_2O at 80 °C for 4 weeks.

temperature for all PILs, attributed to a water-assisted ion transport mechanism. The activation energy of the PILs with 5-, 6-, 7-, 8-, and 9-membered ring cations were 29.4, 44.3, 35.7, 40.9, and 55.9 kJ mol^{-1}, respectively. At 80 °C and 90% RH, the conductivity reaches values of 19.2, 19.0, 15.9, 6.8, and 3.8 mS cm^{-1} (MPyr > MPip > MAzp > MAzc > MAzn). Water uptake (Figure 3b) remains relatively constant with increasing temperature (30−60 °C) at 90% RH for all PILs. At each temperature, water uptake increases with decreasing cation size (MPyr > MPip > MAzp > MAzc > MAzn), a similar order to conductivity values. The water uptake of poly(VBMPyr-Br)-5 (ca. 41 wt %) is more than 2-fold higher than poly(VBMAzn-Br)-9 (ca. 18 wt %). The difference in the water uptake may be attributed to the increase in hydrophobicity with increasing ring size (increasing number of methylene groups per ring).

Figure 3c,d shows the bromide ion conductivity and water uptake, respectively, of the PILs as a function of relative humidity at a constant temperature of 60 °C. Note that the conductivity of poly(VBMAzn-Br)-9 was obtained only at 75% and 90% RH as the film was too brittle below 60% RH to obtain accurate conductivity measurements. As expected, the conductivity (Figure 3c) increases with increasing relative humidity for all PILs, where the conductivities at 90% RH are approximately 2 orders of magnitude higher than those at 45% RH for PILs with 5-, 6-, 7-, and 8-membered ring cations. This again provides evidence of the water-assisted ion transport mechanism, where the water uptakes increase over 3-fold from 45% to 90% RH for all PILs (e.g., highest increase: poly(VBMPyr-Br)-5, 9.6 wt % to 39.9 wt %; lowest increase: poly(VBMAzc-Br)-9, 5.7 wt % to 18.5 wt %). The conductivity difference between PILs with different cation ring sizes decreases with increasing humidity. For example, at 45% RH, conductivity of poly(VBMPyr-Br)-5 is 3 orders of magnitude higher than that of poly(VBMAzc-Br)-8, whereas at 90% RH, conductivity of poly(VBMPyr-Br)-5 is less than 1 order of magnitude higher than that of poly(VBMAzc-Br)-8. A summary of the ion conductivities and water uptakes of the PILs at 60 °C and 90% RH are listed in Table 1.

In order to provide deeper insights into the impact of water uptake on ion conductivity, the ion conductivity was plotted as

DOI: 10.1021/acsmacrolett.9b00039
ACS Macro Lett. 2019, 8, 540−545

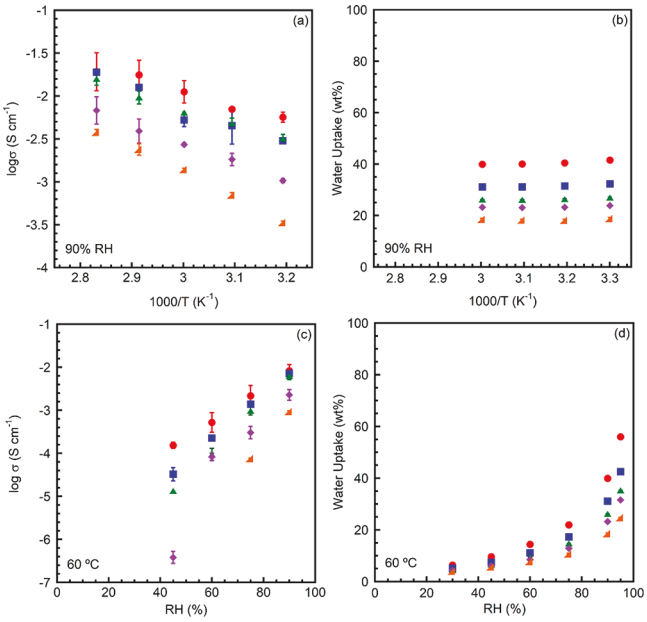

Figure 3. Temperature-dependent (a) ion conductivity and (b) water uptake at 90% RH and humidity-dependent (c) ion conductivity and (d) water uptake at 60 °C for bromide-conducting PILs: poly(VBMPyr-Br)-5 (red circles), poly(VBMPip-Br)-6 (blue squares), poly(VBMAzp-Br)-7 (green triangles), poly(VBMAzc-Br)-8 (purple diamonds), and poly(VBMAzn-Br)-9 (orange triangles).

a function of hydration number (λ, mol H_2O/mol cation) of the PILs (Figure 4a) and the volume fraction of water in the PILs (Figure 4b) at 60 °C. Figure 4a shows that the bromide conductivity increases with increasing hydration number of the PILs, where a master curve (power law) can be regressed to all PILs, indicating a universal scaling of the conductivity with the water content, regardless of the cation ring sizes. When the hydration number is higher than 1, the conductivity started to increase significantly with hydration number, suggesting a change in the connectivity of the ion conducting pathways of the PILs (similar to percolation theory). Figure 4b shows the bromide conductivity as a function of the volume fraction of water in PILs. Details on the calculation of volume fraction are described in the Supporting Information. The data in Figure 4b was regressed to percolation theory (eq 1), where a master curve (universal scaling) was also observed for all PILs regardless of cation size.

$$\sigma = \sigma_0(\phi_w - \phi_c)^{\gamma_D} \quad (1)$$

In eq 1, σ is the overall bromide conductivity of the PILs, σ_0 is the inherent conductivity, ϕ_c is the critical volume fraction (volume fraction at the percolation threshold), and γ_D is a critical exponent, which depends on the geometric organization of the connected conductive ionic network. The critical

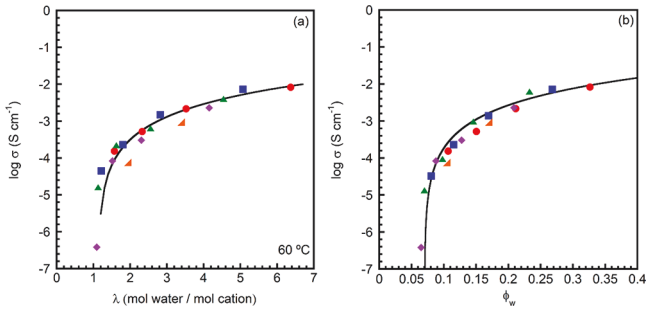

Figure 4. Bromide ion conductivity vs (a) hydration number and (b) volume fraction of water at 60 °C for PILs: poly(VBMPyr-Br)-5 (red circles), poly(VBMPip-Br)-6 (blue squares), poly(VBMAzp-Br)-7 (green triangles), poly(VBMAzc-Br)-8 (purple diamonds), and poly(VBMAzn-Br)-9 (orange triangles).

volume fraction was determined to be approximately 0.07 for all PILs regardless of cation ring size, i.e., percolation threshold is the same for all PILs regardless of cation ring size. The critical exponents were determined to be 2.17, 2.37, 2.33, and 2.31 for PILs with 5-, 6-, 7-, and 8-membered ring cations, respectively; expected values for a random distribution of percolating conducting domains. The fitting parameters from the percolation theory regression for all PILs are listed in Table S3.

In summary, we report the synthesis of five styrene-based PILs containing saturated *N*-heterocyclic cations with various ring sizes (i.e., methylpyrrolidinium, methylpiperidinium, methylazepanium, methylazocanium, and methylazonanium). For PILs with 5-, 6-, 7-, and 8-membered ring cations, high alkaline chemical stability was observed after 4 weeks in 40 mol equiv of KOH (1.0 M in D_2O) at 80 °C. In addition, the ion conductivity follows percolation theory, where conductivity versus water volume fraction for all the PILs is similar, regardless of the cation ring size, that is, master curve. At 80 °C and 90% RH, a high bromide conductivity of 19.2 mS cm^{-1} was observed for the PIL with a 5-membered ring cation (i.e., poly(VBMPyr-Br)-5) with about 6.3 mol water/mol cation. These results provide further insight on incorporating styrene-based PILs containing saturated *N*-heterocyclic cations as novel building blocks for anion exchange membranes.

■ ASSOCIATED CONTENT

Supporting Information

The Supporting Information is available free of charge on the ACS Publications website at DOI: 10.1021/acsmacrolett.9b00039.

Materials, synthesis, experimental procedures, the thermal property of the PILs, and the percolation theory results (PDF)

Table 1. Ion Conductivity, Water Uptake, and Degree of Degradation of PILs

polymers	σ^a (mS cm^{-1})	water uptake^a (wt %)	λ (mol H_2O/mol cation)	calcd IEC^b (mmol g^{-1})	degree of degradation (%)
poly(VBMPyr-Br)-5	11.2	39.9	6.3	3.5	
poly(VBMPip-Br)-6	5.3	31.1	5.1	3.4	
poly(VBMAzp-Br)-7	6.4	26.2	4.5	3.2	
poly(VBMAzc-Br)-8	2.7	23.2	4.2	3.1	2.2
poly(VBMAzn-Br)-9	1.4	18.5	3.4	3.0	22.2

^{a}Conductivity and water uptake were measured at 60 °C and 90% RH. ^{b}IEC = ion exchange capacity.

DOI: 10.1021/acsmacrolett.9b00039
ACS Macro Lett. 2019, 8, 540−545

AUTHOR INFORMATION

Corresponding Author

*E-mail: elabd@tamu.edu.

ORCID

Yossef A. Elabd: 0000-0002-7790-9445

Notes

The authors declare no competing financial interest.

ACKNOWLEDGMENTS

This work is supported in part by the National Science Foundation under Grant No. CBET-1703645.

REFERENCES

(1) Varcoe, J. R.; Slade, R. C. T. Prospects for Alkaline Anion-Exchange Membranes in Low Temperature Fuel Cells. *Fuel Cells* **2005**, *5*, 187−200.

(2) Merle, G.; Wessling, M.; Nijmeijer, K. Anion exchange membranes for alkaline fuel cells: A review. *J. Membr. Sci.* **2011**, *377*, 1−35.

(3) Hagesteijn, K. F. L.; Jiang, S.; Ladewig, B. P. A review of the synthesis and characterization of anion exchange membranes. *J. Mater. Sci.* **2018**, *53*, 11131−11150.

(4) Dang, H.-S.; Weiber, E. A.; Jannasch, P. Poly(phenylene oxide) functionalized with quaternary ammonium groups via flexible alkyl spacers for high-performance anion exchange membranes. *J. Mater. Chem. A* **2015**, *3*, 5280−5284.

(5) Dong, X.; Lv, D.; Zheng, J.; Xue, B.; Bi, W.; Li, S.; Zhang, S. Pyrrolidinium-functionalized poly(arylene ether sulfone)s for anion exchange membranes: Using densely concentrated ionic groups and block design to improve membrane performance. *J. Membr. Sci.* **2017**, *535*, 301−311.

(6) Mohanty, A. D.; Ryu, C. Y.; Kim, Y. S.; Bae, C. Stable Elastomeric Anion Exchange Membranes Based on Quaternary Ammonium-Tethered Polystyrene-b-poly(ethylene-co-butylene)-b-polystyrene Triblock Copolymers. *Macromolecules* **2015**, *48*, 7085−7095.

(7) Dang, H.-S.; Jannasch, P. A comparative study of anion-exchange membranes tethered with different hetero-cycloaliphatic quaternary ammonium hydroxides. *J. Mater. Chem. A* **2017**, *5*, 21965−21978.

(8) Fang, J.; Wu, Y.; Zhang, Y.; Lyu, M.; Zhao, J. Novel anion exchange membranes based on pyridinium groups and fluoroacrylate for alkaline anion exchange membrane fuel cells. *Int. J. Hydrogen Energy* **2015**, *40*, 12392−12399.

(9) Gu, F.; Dong, H.; Li, Y.; Sun, Z.; Yan, F. Base Stable Pyrrolidinium Cations for Alkaline Anion Exchange Membrane Applications. *Macromolecules* **2014**, *47*, 6740−6747.

(10) Ye, Y.; Sharick, S.; Davis, E. M.; Winey, K. I.; Elabd, Y. A. High Hydroxide Conductivity in Polymerized Ionic Liquid Block Copolymers. *ACS Macro Lett.* **2013**, *2*, 575−580.

(11) Olsson, J. S.; Pham, T. H.; Jannasch, P. Poly(N,N-diallylazacycloalkane)s for Anion-Exchange Membranes Functionalized with N-Spirocyclic Quaternary Ammonium Cations. *Macromolecules* **2017**, *50*, 2784−2793.

(12) Pham, T. H.; Olsson, J. S.; Jannasch, P. N-Spirocyclic Quaternary Ammonium Ionenes for Anion-Exchange Membranes. *J. Am. Chem. Soc.* **2017**, *139*, 2888−2891.

(13) Nuñez, S. A.; Capparelli, C.; Hickner, M. A. N-Alkyl Interstitial Spacers and Terminal Pendants Influence the Alkaline Stability of Tetraalkylammonium Cations for Anion Exchange Membrane Fuel Cells. *Chem. Mater.* **2016**, *28*, 2589−2598.

(14) Arges, C. G.; Wang, L.; Parrondo, J.; Ramani, V. Best Practices for Investigating Anion Exchange Membrane Suitability for Alkaline Electrochemical Devices: Case Study Using Quaternary Ammonium Poly(2,6-dimethyl 1,4-phenylene)oxide Anion Exchange Membranes. *J. Electrochem. Soc.* **2013**, *160*, F1258−F1274.

(15) Amel, A.; Zhu, L.; Hickner, M.; Ein-Eli, Y. Influence of Sulfone Linkage on the Stability of Aromatic Quaternary Ammonium Polymers for Alkaline Fuel Cells. *J. Electrochem. Soc.* **2014**, *161*, F615−F621.

(16) Nuñez, S. A.; Hickner, M. A. Quantitative ^{1}H NMR Analysis of Chemical Stabilities in Anion-Exchange Membranes. *ACS Macro Lett.* **2013**, *2*, 49−52.

(17) Ye, Y. S.; Elabd, Y. A. Relative Chemical Stability of Imidazolium-Based Alkaline Anion Exchange Polymerized Ionic Liquids. *Macromolecules* **2011**, *44*, 8494−8503.

(18) Chen, D.; Hickner, M. A. Degradation of Imidazolium- and Quaternary Ammonium-Functionalized Poly(fluorenyl ether ketone sulfone) Anion Exchange Membranes. *ACS Appl. Mater. Interfaces* **2012**, *4*, 5775−5781.

(19) Mohanty, A. D.; Tignor, S. E.; Krause, J. A.; Choe, Y.-K.; Bae, C. Systematic Alkaline Stability Study of Polymer Backbones for Anion Exchange Membrane Applications. *Macromolecules* **2016**, *49*, 3361−3372.

(20) Sun, Z.; Lin, B.; Yan, F. Anion-Exchange Membranes for Alkaline Fuel-Cell Applications: The Effects of Cations. *ChemSusChem* **2018**, *11*, 58−70.

(21) Meek, K. M.; Elabd, Y. A. Alkaline Chemical Stability of Polymerized Ionic Liquids with Various Cations. *Macromolecules* **2015**, *48*, 7071−7084.

(22) Meek, K. M.; Nykaza, J. R.; Elabd, Y. A. Alkaline Chemical Stability and Ion Transport in Polymerized Ionic Liquids with Various Backbones and Cations. *Macromolecules* **2016**, *49*, 3382−3394.

(23) Sturgeon, M.; Macomber, C.; Engtrakul, C.; Long, H.; Pivovar, B. Hydroxide based Benzyltrimethylammonium Degradation: Quantification of Rates and Degradation Technique Development. *J. Electrochem. Soc.* **2015**, *162*, F366−F372.

(24) Belhocine, T.; Forsyth, S. A.; Gunaratne, H. Q. N.; Nieuwenhuyzen, M.; Puga, A. V.; Seddon, K. R.; Srinivasan, G.; Whiston, K. New ionic liquids from azepane and 3-methylpiperidine exhibiting wide electrochemical windows. *Green Chem.* **2011**, *13*, 59−63.

(25) Belhocine, T.; Forsyth, S. A.; Gunaratne, H. Q. N.; Nieuwenhuyzen, M.; Nockemann, P.; Puga, A. V.; Seddon, K. R.; Srinivasan, G.; Whiston, K. Azepanium ionic liquids. *Green Chem.* **2011**, *13*, 3137−3155.

(26) De Rycke, N.; David, O.; Couty, F. Assessing the Rates of Ring-Opening of Aziridinium and Azetidinium Ions: A Dramatic Ring Size Effect. *Org. Lett.* **2011**, *13*, 1836−1839.

(27) Meek, K. M.; Sun, R.; Willis, C.; Elabd, Y. A. Hydroxide conducting polymerized ionic liquid pentablock terpolymer anion exchange membranes with methylpyrrolidinium cations. *Polymer* **2018**, *134*, 221−226.

(28) Ponce-González, J.; Whelligan, D. K.; Wang, L.; Bance-Soualhi, R.; Wang, Y.; Peng, Y.; Peng, H.; Apperley, D. C.; Sarode, H. N.; Pandey, T. P.; Divekar, A. G.; Seifert, S.; Herring, A. M.; Zhuang, L.; Varcoe, J. R. High performance aliphatic-heterocyclic benzyl-quaternary ammonium radiation-grafted anion-exchange membranes. *Energy Environ. Sci.* **2016**, *9*, 3724−3735.

(29) Marino, M. G.; Kreuer, K. D. Alkaline Stability of Quaternary Ammonium Cations for Alkaline Fuel Cell Membranes and Ionic Liquids. *ChemSusChem* **2015**, *8*, 513−523.

(30) Jiang, Y.; Liao, J.; Yang, S.; Li, J.; Xu, Y.; Ruan, H.; Sotto, A.; Van der Bruggen, B.; Shen, J. Stable cycloaliphatic quaternary ammonium-tethered anion exchange membranes for electrodialysis. *React. Funct. Polym.* **2018**, *130*, 61−69.

DOI: 10.1021/acsmacrolett.9b00039
ACS Macro Lett. 2019, 8, 540−545